13th International Symposium on Turbulence and Shear Flow Phenomena (TSFP13)
Montreal, Canada, June 25–28, 2024

ON THE STRUCTURE AND BEHAVIOUR OF THE WAKE BEHIND A THREE-DIMENSIONAL HILL

Daniel MacGregor and Philippe Lavoie
Institute for Aerospace Studies
University of Toronto
4925 Dufferin St., Toronto, Ontario, M3H 5T6, Canada
daniel.macgregor@mail.utoronto.ca, phil.lavoie@utoronto.ca

ABSTRACT

Experiments to characterize the bi-stable wake of a three-dimensional hill geometry were conducted at the University of Toronto Institute for Aerospace Studies. The switching between bi-stable modes was captured through unsteady surface-pressure measurements. The timescales between switching events matches with an exponential distribution showing that this is a random process and not a periodic phenomena. The mean switch time is in the order of 10^3 convective timescales and varies non-monotonically with Reynolds number. The bi-stable behaviour is present over an approximately 4° range of hill orientation. Flow field measurements of the wake were captured using stereoscopic particle image velocimetry. There is a decreases in the size of the recirculation region with increasing Reynolds number along with a shift in the separation point of the shear layer from the side of the hill. The shear layer from the sides of the hill meet downstream of the recirculation region to form a single streamwise vortex. The flow field results are used to create a schematic of the wake.

INTRODUCTION

The Benchmark Validation Experiments for RANS and LES Investigations (BeVERLI) was designed as part of a project concerned with three-dimensional non-equilibrium turbulent boundary layers that are subjected to a combination of surface curvature and pressure gradient effects (Gargiulo *et al.*, 2020, 2021). These effects are generated by a three-dimensional hill geometry, which provides a simple experimental setup that can be used to collect benchmark datasets for use with computational groups to improve modelling capabilities for these flows.

Previous work with the BeVERLI hill by Duetsch-Patel *et al.* (2022) found that the wake at hill orientation of 0° was asymmetric and bi-stable. The bi-stable behaviour was observed in independent experiments conducted at SINTEF and VT. This phenomena was explored in greater details by MacGregor *et al.* (2023) through unsteady surface-pressure measurements over the leeward face of the hill. The timescale between switching events of the wake was on average of the order of $10^3 \cdot h/U_\infty$, where h is the model height and U_∞ is the freestream velocity. Conditionally averaged mean surface-pressure fields for the bi-stable modes found them to have mirror symmetry about the model centerline.

Similar bi-stable wake behaviours have been observed with other geometries including a rearward facing double step (Herry *et al.*, 2011), simplified ship geometries (Zhu *et al.*, 2023) and the Ahmed body (Grandemange *et al.*, 2013). Grandemange *et al.* (2013) characterized the bi-stable wake of an Ahmed body and found it was independent of Reynolds number and dependent on the ground clearance under the body. Switching between bi-stable modes was found to be random in nature with the average timescale between switching events to be on the order of $10^3 \cdot \ell/U_\infty$, where ℓ is the height of the Ahmed body. More recent work by Haffner *et al.* (2020), provided insight into the shear layer interaction from the Ahmed body and how they influence the bi-stable modes and its switching. The previously studied geometries that show bi-stable wake behaviour all have sharp trailing edges giving fixed points of separation, whereas the BeVERLI hill is a smooth curved geometry allowing for the movement of the separation point with changing flow conditions.

The objective of this paper is to expand on the work by MacGregor *et al.* (2023) through additional unsteady surface-pressure to further characterize the bi-stable wake behaviour, and flow field measurements to identify the primary features that compose the wake. These results are compared against the bi-stable wake behaviour seen on other geometries.

EXPERIMENTAL SETUP

The BeVERLI hill is defined using a fifth-degree polynomial to give a curve that rises a height, h, to a flat region of width $0.5h$ before descending using the same curve for an overall width of $5h$. The polynomial has constraints set in its first and second derivatives to facilitate smooth transitions in curvature between flat regions. This profile is extruded to a width of $0.5h$. It is then traced along a modified super-elliptic curve such that it has symmetry every 90° when rotated about the centre vertical axis. A more detailed description of the BeVERLI hill design is provided by Gargiulo *et al.* (2020).

For experiments at UTIAS, a scaled version of the hill with height $h = 0.12$ m was used. One half of the hill has a dense distribution of pressure ports in lines extending radially from the model centre in 15° increments, and the other half has similar lines of taps at 45° increments. Figure 1b shows this pressure port distribution. The model was integrated into a circular base to simplify changes in orientation. The model was machined from a single block of 6061 aluminum and anodized in a matte black finish.

Experiments were conducted using the recirculating wind tunnel at UTIAS. This tunnel has a cross-sectional area that is 1.2 m wide by 0.8 m tall with an overall length of 5 m. The tunnel is capable of producing flow speeds up to 35 m/s with

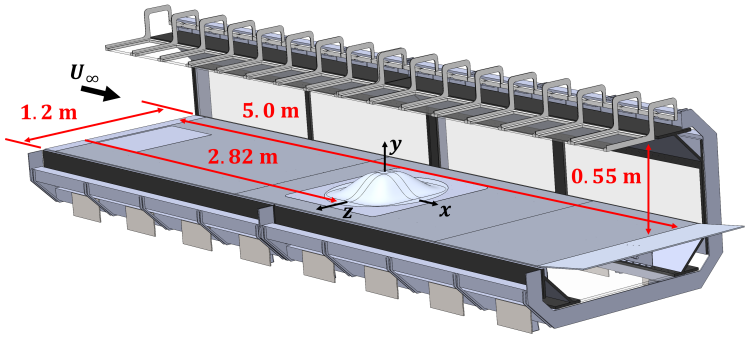

(a) Schematic of experimental setup.

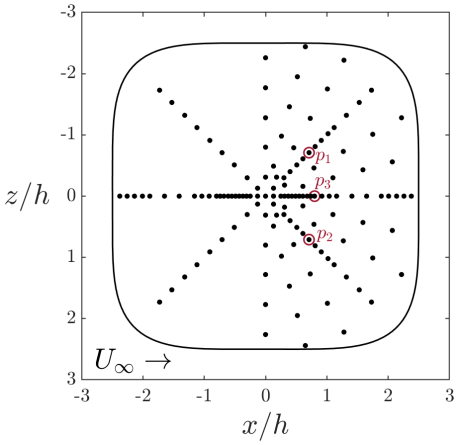

(b) Pressure port distribution.

Figure 1: (a) Schematic of experimental with global coordinate system shown, and (b) the distribution of pressure ports with the Endevco ports identified.

free stream turbulence intensities peaking at 0.08% at maximum speed. The hill model is located 2.8 m downstream from the leading edge of a boundary layer plate setup that extends the full length of the test section. This setup reduces the testing cross-sectional area to 1.2 m by 0.55 m. The test section and plate are adjusted such that a zero-pressure-gradient turbulent boundary layer approaches the hill with a zero-pressure-gradient recovery region downstream of the hill. A zig-zag trip was placed 60 mm downstream from the leading edge of the plate to promote a boundary layer transition.

The coordinate system used is defined with the x-axis aligned with the freestream velocity, U_∞, and the origin is located at the centre of the hill co-planar with the surface of the boundary layer plate. The y-axis is oriented normal to the boundary layer plate and extends through the flat top of the hill, and is used to define rotations of the hill. An orientation of 0° is defined such that the surface normal from the extruded polynomial profile and the freestream vector are co-planar. From this definition, the hill will have unique orientations from 0° to 45° with orientations between 45° to 90° being mirror symmetric of those from 45° to 0°, respectively. A view of the UTIAS experimental setup with the defined coordinate system and the hill at 0° can be found in Figure 1a.

For the present experiments, the model height based Reynolds number, Re_h, ranged from 38,000 to 250,000. The boundary layer height, δ, to model height ratio, δ/h, ranged from 0.4 at $\mathrm{Re}_h = 80,000$ to 0.34 at $\mathrm{Re}_h = 250,000$. With the current experimental setup, a change in Reynolds number is coupled with a change in the δ/h ratio. For the present work, the change in Re_h is an order of magnitude whereas the change in δ/h is only about 15%. Thus, Re_h is assumed to be the primary factor driving changes in the flow.

Unsteady surface-pressure measurements were collected using Endevco 1 psig transducers connected at the end of approximately 20 cm lengths of 1/16 inch diameter Tygon tubing. Tubes of these lengths were used to minimize any pressure signal attenuation and lag effects. Three sensors were connected to the ports indicated in Figure 1b. Pressure signals were collected at 25 kHz and digitally filtered using a moving average filter with window width of 0.002 s giving a cutoff frequency of 90 Hz.

Flow field measurements were collected using stereoscopic particle image velocimetry (PIV). The flow was seeded with Bis(2-ethylhexyl) sebacate to give particles 1 μm in diameter. The seeded flow was illuminated using an Evergreen dual pulse 532 nm ND:Yag laser with 200 mJ per pulse with a series of optic lenses to form a 1 mm thick light sheet. Particle images were acquired using two sCMOS Lavision cameras and a Lavision Programmable Timinig Unit (PTU). The collected images were processed using Davis 8 software to give the vector fields, which were exported to MATLAB for additional analysis.

RESULTS

Bi-stable Switching

As discussed earlier, the wake of the BeVERLI hill at 0° was found to switch between two quasi-stable modes that are mirror symmetric about the hill centerline. The two bi-stable modes are denoted as $\mathscr{P}$ and $\mathscr{N}$, where for the $\mathscr{P}$ mode, the maximum streamwise extent of the recirculation region is positioned on the $+z$ side of the hill and vice versa for the $\mathscr{N}$ mode.

The state of the bi-stable wake was tracked through the surface-pressure signals p_1 and p_2 collected at the locations shown in Figure 1b. A methodology adapted from Plumejeau *et al.* (2019) was created that uses these two signals to calculate a non-dimensional parameter $r = (p_2 - p_1)/(p_2 + p_1)$. This signal is centred about zero so that positive r indicates that the wake is in the $\mathscr{P}$ mode and vice versa for the $\mathscr{N}$ case.

A switching event between modes was taken to be an instance where r passes zero by an amount at least 85% of the magnitude of r when in the new bi-stable mode. A portion of the time series of r for $\mathrm{Re}_h = 123,000$ is shown in Figure 2a. In this plot, the time, t, is non-dimensionalized by the freestream velocity, U_∞, and hill height h. The vertical dotted lines indicate switching events of the bi-stable wake under the methodology described. Instances where r crossed zero but did not meet the threshold criteria can also be seen, for example between $tU_\infty/h \in [0, 1000]$. Given the bi-stable nature of the wake, mean statistics of the measurements would not provide a meaningful representation of the flow. Instead, conditional averaging based on the bi-stable modes is required to build a more accurate description of this flow.

The time elapsed between the bi-stable mode switching events, t_s, was tracked using the identified switches in the r signals. The probability density function (PDF) of t_s is shown in Figure 2b. This plot also includes an exponential distribution

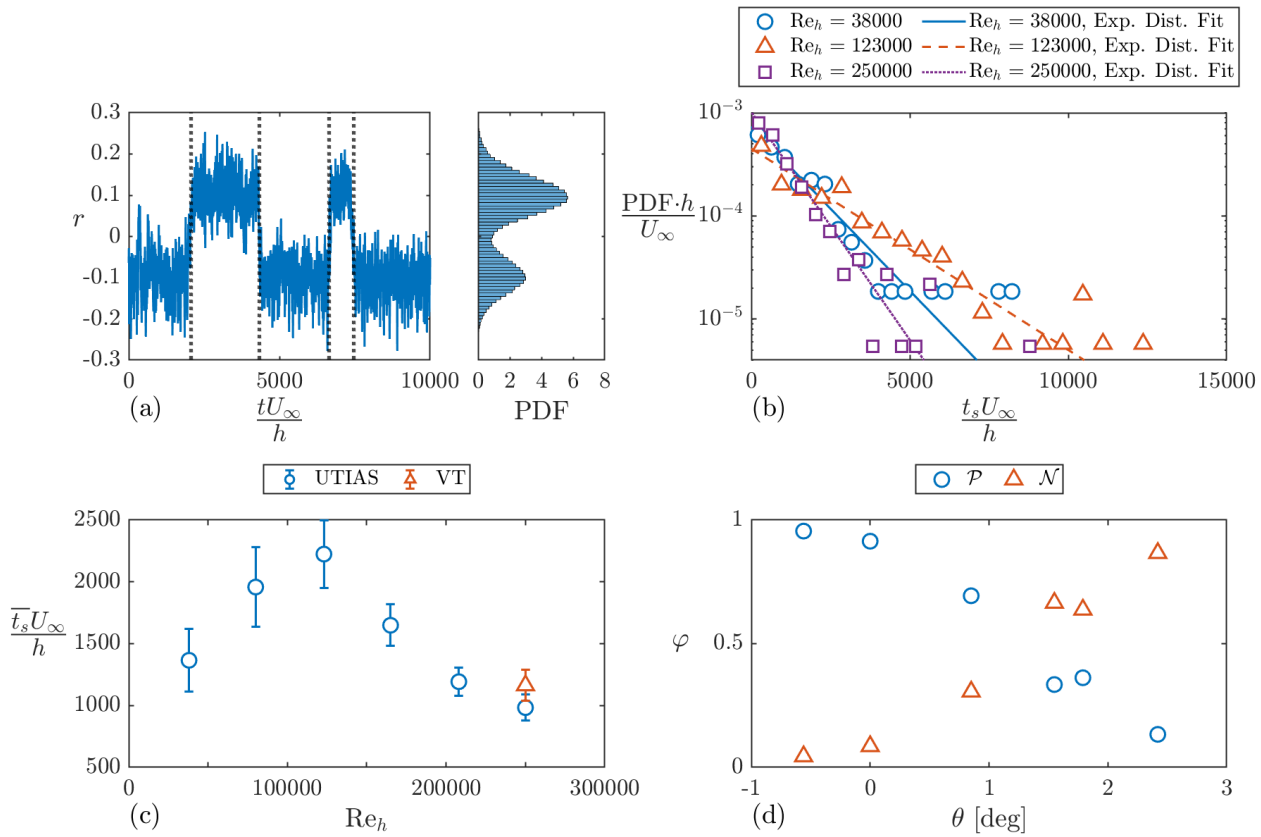

Figure 2: (a) sample of r for $\mathrm{Re}_h = 123{,}000$ (full signal not shown) with switching events of the bi-stable wake indicated by vertical dotted lines, and a histogram of r, (b) PDF of t_s for different Re_h with corresponding exponential distributions, (c) mean switch time, $\overline{t_s}$, for the range of Reynolds numbers tested, and (d) ratio of $\mathscr{P}$ and $\mathscr{N}$ for small changes in the hill orientation from 0° for $\mathrm{Re}_h = 123{,}000$.

based on the mean average switching time for each Reynolds number. The agreement of the data with their respective exponential distributions shows that the bi-stable switching is a Poison process. This is a critical result as it establishes that these events are random in nature and do not occur as a periodic phenomena. Furthermore, the lack of collapse across the Reynolds numbers indicates that the bi-stability shares a Reynolds number dependency. This dependency can be seen in Figure 2c, where there is a non-monotonic relation between $\overline{t_s}$ and Reynolds number. The $\overline{t_s}U_\infty/h$ collected by MacGregor *et al.* (2023) at Virginia Tech using the same physical geometry for $Re_h = 250{,}000$ is also included and found to match within measurement errors to the measurements taken at UTIAS. This plot also shows that the flow can remain on average in any one bi-stable mode for 10^3 convective timescales.

These findings share some similarity to those made by Grandemange *et al.* (2013) with the Ahmed body. First, the switching behaviour of the bi-stable wake for both bodies follows a Poison point process. Next, the large time scale between switching events is seen with both geometries. An area of difference is in the Reynolds number dependence of the bi-stable behaviour seen with the BeVERLI hill, which was not found with the Ahmed body.

Sensitivity of the Bi-stability

Let φ denote the fraction time that the wake was in one of the bi-stable modes. It would be expected with the hill at 0° that φ would be evenly split between $\mathscr{P}$ and $\mathscr{N}$. An even split was not observed in experiments with the wake consistently being biased toward the $\mathscr{P}$ mode (see the histogram in Figure 2a). This biasing reflects the sensitivity of the bi-stability to variations in boundary conditions and small non-uniformities with the inflow conditions. Furthermore, minor deviations in the setup between experiments can change the ratio seen with the hill mounted at 0°. For example, the $\mathscr{P}$ to $\mathscr{N}$ ratio was tracked in two separate experimental entries where a 70% to 30% split and a 90% to 10% split, respectively, was observed. The histogram of r for the 70% to 30% split at $\mathrm{Re_h} = 123{,}000$ is shown in the histogram of Figure 2a.

The change in φ was tracked over a range of small angle adjustments to the hill orientation from 0°, which is denoted by θ. The hill is considered geometrically at 0° orientation ($\theta = 0°$) when the locating pin was used to align the hill in boundary layer plate setup. The change in φ for a range of angles at $\mathrm{Re}_h = 123{,}000$ is shown in Figure 2d for the experimental entry when the 90% to 10% $\mathscr{P}$ to $\mathscr{N}$ split was observed. As the hill was rotated in the $-\theta$ direction, the bi-stable wake increasingly favoured the $\mathscr{P}$ mode, where with large enough change from 0° the wake would lock into this mode. Conversely, when rotated in $+\theta$ direction, the hill would increasingly favour the $\mathscr{N}$ mode before locking into it at sufficiently large θ. From Figure 2d, the presence of the bi-stability occurs over a narrow range of 4°, with an even split being expected at $\theta \approx 1.3°$. The small range of angles where the wake is bi-stable highlights the sensitivity of this to boundary and inflow conditions. This range of effective angles for the bi-stability is larger than that reported by Haffner *et al.* (2020) with the Ahmed body, where the effective range of the bi-stbale wake was 1.4°.

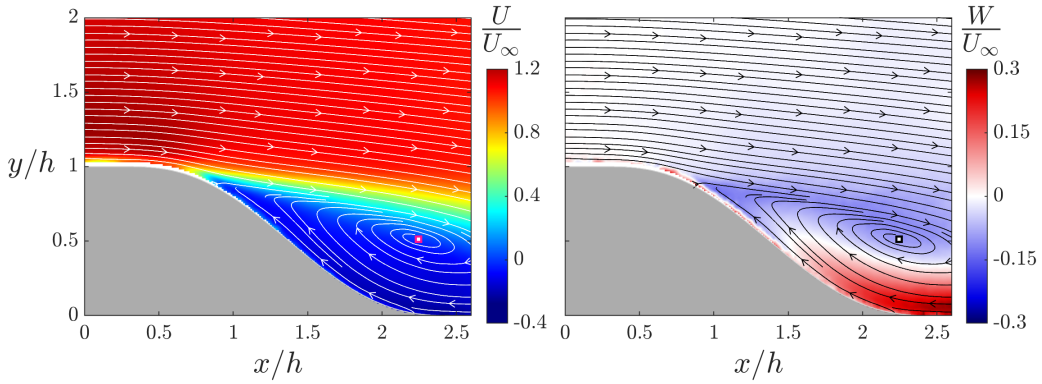

Figure 3: Flow field in the x-y plane at $z/h = 0$ for $\mathrm{Re}_h = 38{,}000$ for the $\mathscr{P}$ bi-stable case. Squares indicate location of focal point based on the U-V streamline pattern. On the left is U/U_∞ and on the right is W/U_∞.

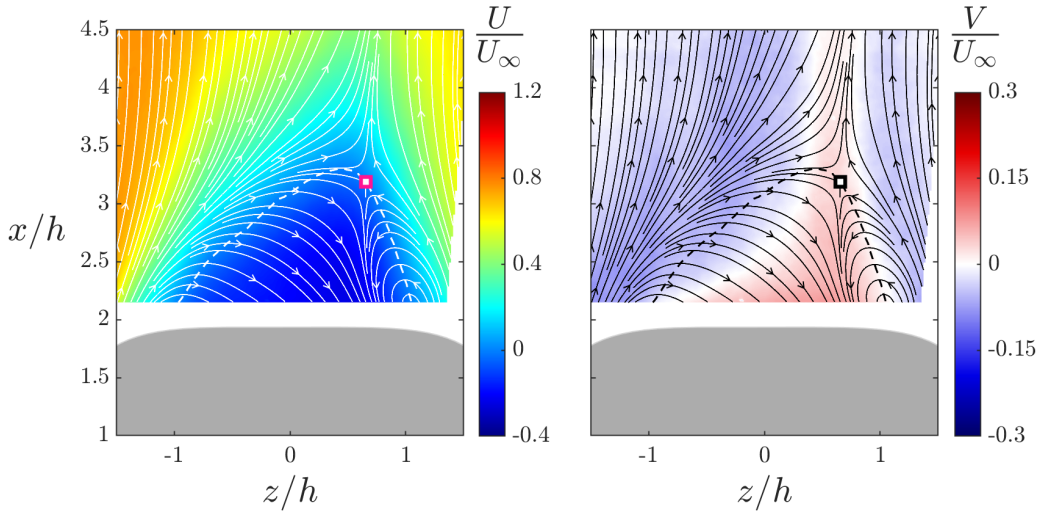

Figure 4: Flow field in the z-x plane at $y/h = 0.1$ for $\mathrm{Re}_h = 38{,}000$ for the $\mathscr{P}$ bi-stable case. Squares indicate location of saddle or focal point based on the U-W streamline pattern. On the left is U/U_∞ and on the right is V/U_∞.

Flow Field

As discussed previously, tracking the bi-stable mode is necessary to generate meaningful results as taking the temporal mean will not reflect this flow accurately. Thus, for all flow field measurements presented, the bi-stable mode was tracked using Endevco pressure transducers at the p_1 and p_2 positions in Figure 1b. Snapshots collected were then conditionally averaged into the $\mathscr{P}$ or $\mathscr{N}$ modes.

The mean streamwise, U, and spanwise, W, velocity components of the $\mathscr{P}$ conditionally averaged snapshots for the x-y plane located at $z/h = 0$ for $\mathrm{Re}_h = 38{,}000$ are presented in Figure 3. The mean U and V velocity components are used to generate a streamline mapping, which illustrate a $-z$ oriented spanwise recircualtion region with focal point at $(x/h, y/h) = (2.3, 0.6)$. Significant spanwise flow is present within the recirculation region indicating that the recirculating flow has streamwise and spanwise components of recirculation. This spanwise flow is equal and opposite in the $\mathscr{N}$ mode, which indicates mirror symmetry between the bi-stable modes as seen in surface-pressure measurements by MacGregor *et al.* (2023). Also, these results match those collected by Duetsch-Patel *et al.* (2022) for the same plane within the wake.

The mean streamwise, U, and wall-normal, V, velocity components of the $\mathscr{P}$ conditionally averaged snapshots for the z-x plane located at $y/h = 0.1, 0.54$ and 0.80 are shown in Figures 4, 5 and 6, respectively. The boundary of the recirculation region, where $U = 0$, is shown for each plane. For the $\mathscr{P}$ mode, the region of negative U extends farther downstream on the $+z$ side of the hill. The U and W components of velocity are used to generate streamline mappings for the z-x flow fields. The location of focus and saddle points in these streamline mappings are indicated by square markers.

At $y/h = 0.1$ (see Figure 4), the recirculation region contains two smaller flows. The larger of these two flows is fed from the shear layer on the $-z$ side of the hill. This flow travels along the hill until its meets the smaller flow, where it then travels up the hill. The line of rotation for the smaller recirculating flow is oriented in the positive wall-normal direction and is centred at $(x/h, z/h) = (2.1, 1.1)$. This region extends upward and toward the model centerline with the core of the recirculating flow being seen as the focus point in Figure 5. At approximately $y/h = 0.5$, this recirculating flow tilts into the $-z$ direction and extends across the recirculation region to the $-z$ side where it hits the hill again. Downstream of the recirculation region, the shear layers from the sides of the hill meet at $z/h = 0.8$ and form an upwash. This motion combined with the strong spanwise flow results in the formation of a streamwise vortex with rotation axis oriented in the $-x$ direction.

Changes in the shape of the recirculation region are explored through the $U = 0$ contour for the $\mathscr{P}$ conditionally averaged snapshots (see Figure 7a). As the Reynolds number increases, the size of the recirculation region decreases with

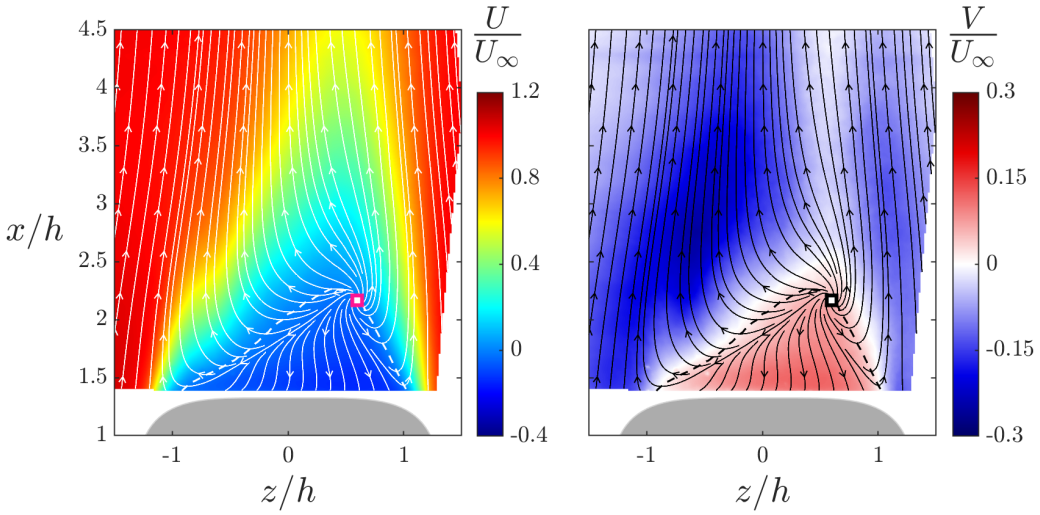

Figure 5: Flow field in the z-x plane at $y/h = 0.54$ for $\mathrm{Re}_h = 38,000$ for the $\mathscr{P}$ bi-stable case. Squares indicate location of saddle or focal point based on the U-W streamline pattern. On the left is U/U_∞ and on the right is V/U_∞.

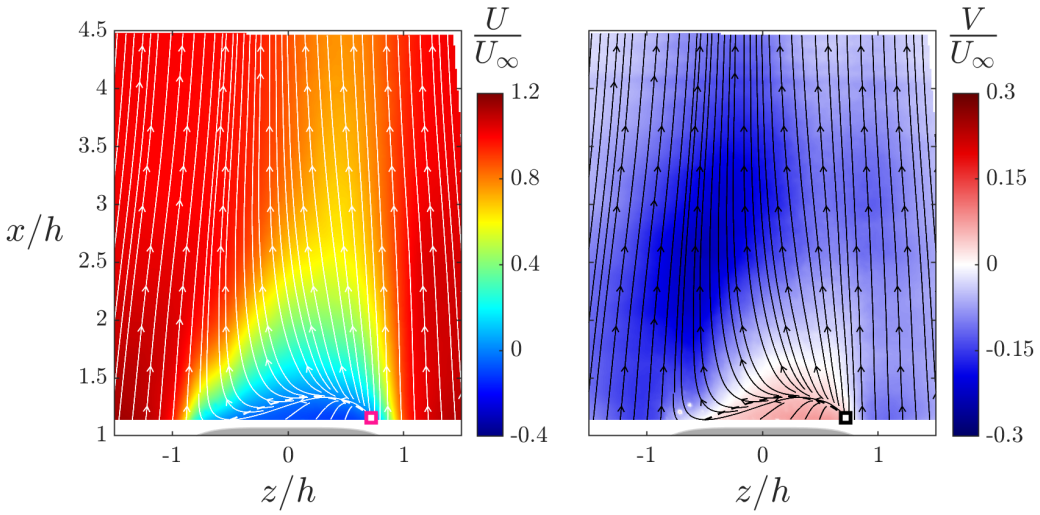

Figure 6: Flow field in the z-x plane at $y/h = 0.80$ for $\mathrm{Re}_h = 38,000$ for the $\mathscr{P}$ bi-stable case. Squares indicate location of saddle or focal point based on the U-W streamline pattern. On the left is U/U_∞ and on the right is V/U_∞.

the sharpest change being from $\mathrm{Re}_h = 38,000$ to $80,000$. The largest change can be seen in $y/h = 0.54$ plane, where the maximum extent of the recirculation region decreases from $x/h = 2.25$ to 2.05 with a reduction in the bulging of the recirculation region at $z/h = 0.45$.

The change in position of the $U = 0$ contour near the hill can also provide insight into any movement of the shear layer separation point. For the $+z$ side of the hill, the start location of the $U = 0$ contour remains unchanged, whereas on the $-z$ side of the hill its position varies with Reynolds number. This can be seen at $y/h = 0.54$ where the starting spanwsie position of the $U = 0$ shifts from $z/h = -0.92$ to $z/h = -0.74$ at $\mathrm{Re}_h = 38,000$ and $165,000$, respectively. This shift in $U = 0$ with increasing Reynolds number indicates that separation on the $-z$ side of the hill is being delayed to a location farther along the hill.

Structure of the Bi-stable wake

The flow field results can be used to visualize the structure of the wake for the $\mathscr{P}$ bi-stable mode. An illustration of the wake structure for this mode is provided in Figure 7b. The $\mathscr{N}$ bi-stable mode would be a mirror-symmetric copy of the sketch shown.

The recirculation region is denoted by the blue region. Near the base of the hill, fluid from the shear layer on the $-z$ side of the hill is entrained and flows across the span of the hill before converging with a smaller $+y$ oriented rotating flow (see Figure 4). The flow is then directed up the hill, while some of the flow near the surface of the hill is pulled into the smaller rotating flow. The line of rotation for the recirculation region, shown as the dashed line, extends up from the wall out of the smaller rotating flow before tilting in the $-x$ and $-z$ directions (see Figures 3 and 5) and into the upper $-z$ side of the hill. This description matches well with the oil flow visualization tests performed by Gargiulo *et al.* (2021). An important consideration to make when comparing these results with those presented is that the oil flow visualization was conducted at a higher Reynolds number and shows the average flow from a single run.

Over the hill, the freestream and shear layer from the hill are directed downwards toward the wall (see Figure 5 and Figure 6). This downward flow is strongest on the $-z$ side, where closer to the wall it turns toward the $z/h = 0.8$ line as seen in

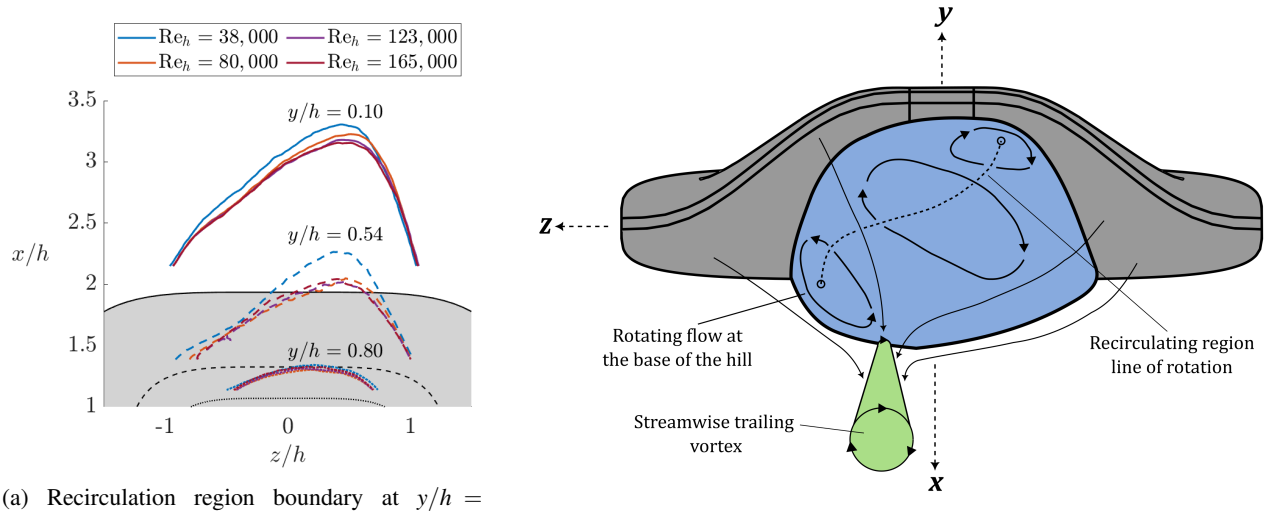

(a) Recirculation region boundary at $y/h = 0.1, 0.54$ and 0.80.

(b)

Figure 7: (a) Recirculation zone boundary, defined as $U = 0$ contour at $y/h = 0.1, 0.54$ and 0.80. (b) sketch of the wake structure for the $\mathscr{P}$ mode.

Figure 4. As discussed previously, this flow meets a similar downward flow from the $+z$ side of the hill creating an upwash. The upwash and strong spanwise flow from the $-z$ side forms a single streamwise vortex with rotation in the $-x$ direction that grows downstream. This vortex is shown as a green cylinder in Figure 7b.

CONCLUSIONS

The flow over the BeVELRI hill presents a case of a bi-stable flow over a geometry with non-sharp trailing edges. Through surface pressure measurements, the switching between the bi-stable cases was found to be a random process and exist over a 4° range of hill orientation. The average switching timescale, $\overline{t_s}$, was found to be greater than $10^3 \cdot h/U_\infty$ for all Reynolds numbers tested. Furthermore, this timescale was found to follow a non-monotonic relation with Reynolds number.

The flow field results presented show that the recirculation region contains two smaller zones near the base of the hill that merge moving up the hill. The recirculation region decreases in size with increasing Reynolds number along with a shift in its shape. The downward flow from opposite sides of the hill meet to create a streamwise oriented vortex that extends downstream. Using the flow field results, a visualization of the bi-stable wake for the $\mathscr{P}$ bi-stable mode is presented.

Future works include the analysis of z-y plane stereoscopic PIV measurements collected at locations downstream of the hill to further the description of the wake. Smoke flow and oil flow visualization tests will also be conducted to complement the flow field results and allow for a more complete picture of the wake dynamics to be made. The behaviour of the bi-stable wake at small orientation changes will be explored further through additional surface-pressure measurements.

REFERENCES

Duetsch-Patel, J. E., MacGregor, D., Jenssen, Y. L., Henry, P.-Y., Muthanna, C., Savio, L., Lavoie, P., Gargiulo, A., Sundarraj, V., Ozoroski, T. A., Devenport, W. J., Borgoltz, A. & Lowe, K. T. 2022 The BeVERLI hill three-dimensional separating flow case: cross-facility comparisons of validation experiment results. In *AIAA SciTech 2022 Forum*. San Diego, CA, USA and Virtual, AIAA–2022–0698.

Gargiulo, A., Beardsley, C., Vishwanathan, V., Fritsch, D. J., Duetsch-Patel, J. E., Szoke, M., Borgoltz, A., Devenport, W. J., Roy, C. J. & Lowe, K. T. 2020 Examination of flow sensitivities in turbulence model validation experiments. In *AIAA SciTech 2020 Forum*. Orlando, FL, USA, AIAA–2020–1583.

Gargiulo, A., Duetsch-Patel, J. E., Ozoroski, T. A., Beardsley, C., Vishwanathan, V., Fritsch, D., Borgoltz, A., Devenport, W. J., Roy, C. J. & Lowe, K. T. 2021 Flow field features of the BeVERLI hill model. In *AIAA Scitech 2021 Forum*. Virtual, AIAA–2021–1741.

Grandemange, M., Gohlke, M. & Cadot, O. 2013 Turbulent wake past a three-dimensional blunt body. Part 1. Global modes and bi-stability. *J. Fluid Mech.* **722**, 51–84.

Haffner, Y., Borée, J., Spohn, A. & Castelain, T. 2020 Mechanics of bluff body drag reduction during transient near-wake reversals. *J. Fluid Mech.* **894** (A14), 1–35.

Herry, B. B., Keirsbulck, L., Labraga, L. & Paquet, J-B. 2011 Flow bistability downstream of three-dimensional double backward facing steps at zero-degree sideslip. *J. Fluids Engineering* **133** (5).

Lowe, Todd, Borgoltz, Aurelien, Devenport, William J, Fritsch, Daniel J, Gargiulo, Aldo, Duetsch-Patel, Julie E, Roy, Christopher J, Szoke, Máté & Vishwanathan, Vidya 2020 Status of the nasa/virginia tech benchmark experiments for cfd validation. In *AIAA SciTech 2020 Forum*, p. 1584.

MacGregor, D. A., Gargiulo, A., Duetsch-Patel, J. E., Lavoie, P. & Lowe, K. T. 2023 Mean and unsteady surface-pressure measurements on the BeVERLI hill. In *AIAA SciTech 2023 Forum*. National Harbor, MD and Virtual, AIAA–2023–0468.

Plumejeau, B., Delprat, S., Keirsbulck, L., Lippert, M. & Abassi, W. 2019 Ultra-local model-based control of the square-back ahmed body wake flow. *Phys. of Fluids* **31** (8), 085103.

Zhu, N., Zhang, Z., Gnanamanickam, E. P. & Leishman, J. G. 2023 Effects of a simulated atmospheric boundary layer on ship airwakes. In *AIAA SCITECH 2023 Forum*. National Harbor, MD, USA and Virtual, AIAA–2023–0470.